Research Article Open Access

Evaluation of the mechanism of the brain transport of nobiletin via passive and P-glycoprotein-mediated transport

Eriko Nakatani[1], Shimako Tanaka[1], Takayuki Yonezawa[2], Je Tae Woo[2], Shizuo Yamada[3], & Takashi Okura[1*]

[1]Laboratory of Pharmaceutics, Faculty of Pharmaceutical Sciences, Teikyo University, Tokyo, Japan; [2]Research Institute for Biological Functions, Chubu University, Kasugai, Aichi, Japan; [3]Center for Pharma-Food Research, Graduate School of Pharmaceutical Sciences, Shizuoka, Japan

***Corresponding Author:** Takashi Okura, Laboratory of Pharmaceutics, Faculty of Pharmaceutical Sciences, Teikyo University, 2-11-1 Kaga, Itabashi-ku, Tokyo 173-8605, Japan

Submission Date: January 13th, 2026; **Acceptance Date:** February 25th, 2026; **Publication Date:** February 27th, 2026

Please cite this article as: Nakatani E., Tanaka S., Yonezawa T., Woo J. T., Yamada S., Okura T. Evaluation of the mechanism of the brain transport of nobiletin via passive and P-glycoprotein-mediated transport. *Functional Foods in Health and Disease.* 2026; 16(2): 181 – 193. DOI: https://doi.org/10.31989/ffhd.v16i2.1888

ABSTRACT

Background: Nobiletin, a polymethoxyflavonoid found in citrus fruits, exhibits neuroprotective potential in disorders of the central nervous system. However, the precise mechanism governing its passage across the blood-brain barrier (BBB) remains unclear.

Objective: This study aimed to elucidate the mechanism of the brain transport of nobiletin by determining its passive transport ability, P-glycoprotein (P-gp) substrate recognition, and the effect of P-gp on its brain transport.

Methods: The ability of nobiletin to traverse the BBB was assessed using an artificial lipid membrane (PAMPA-BBB) to determine passive diffusion parameters. Its interaction with P-gp was examined through ATPase activation assays and bidirectional transport studies in P-gp-overexpressing cell lines (LLC-GA5-COL300) compared with control cells (LLC-PK1). The in vivo distribution of nobiletin in mouse brain and plasma was further quantified following oral administration, with and without P-gp inhibition by elacridar.

Results: Nobiletin exhibited high passive transport in artificial lipid membrane permeation assay. It increased ATPase activity in P-gp-overexpressing membranes. Significant increases in basolateral-to-apical transport were observed in P-gp-expressing cells, indicating that P-gp transports nobiletin as a substrate, similar to verapamil, but not as effectively as

quinidine. When orally administered to mice, the plasma and brain concentrations of nobiletin increased simultaneously and peaked at 30 min, indicating rapid distribution between the blood and brain. The brain/plasma concentration ratio at 30 min was not significantly increased upon P-gp inhibition, indicating that P-gp does not affect the brain transport of nobiletin.

Novelty: This study provides the first quantitative in vivo evidence that P-gp does not functionally restrict the brain distribution of nobiletin, establishing passive diffusion as the predominant BBB transport mechanism of nobiletin.

Conclusions: These results demonstrate that nobiletin efficiently crosses the BBB primarily via passive diffusion, with minimal modulation by P-gp. These findings clarify its brain transport kinetics and reinforce its potential as a neuroprotective bioactive compound for dietary and pharmaceutical development.

Keywords: Nobiletin; Blood–brain barrier; P-glycoprotein; Passive transport; Brain distribution.

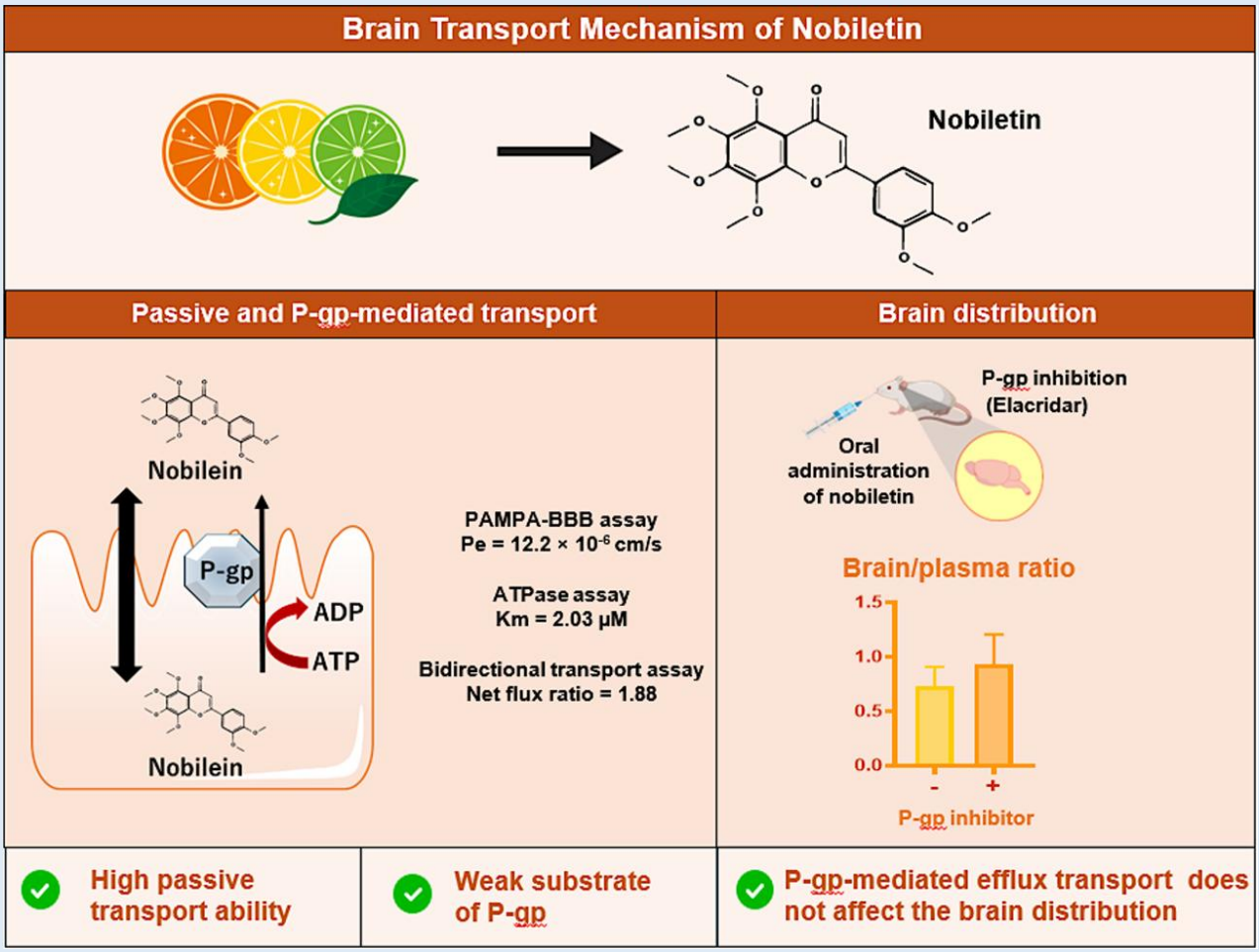

Graphical Abstract: Evaluation of the mechanism of the brain transport of nobiletin via passive and p-glycoprotein-mediated transport.

INTRODUCTION

Nobiletin (3,5,6,7,8,3′,4′-heptamethoxyflavone) is a polymethoxyflavonoid predominantly present in citrus peels [1,2]. This compound exhibits a wide spectrum of biological activities, including anti-inflammatory [3], anticancer [4,5], and antioxidant properties [6]. Beyond these systemic effects, nobiletin has been shown to exert neuroprotective actions that are relevant to neurodegenerative disorders such as Alzheimer's and Parkinson's diseases [7–10]. Clinical evidence also indicates that supplementation with nobiletin-rich extracts may enhance cognitive and memory performance in elderly individuals [11]. Because nobiletin has promising potential in neurological health, its effective delivery to the central nervous system (CNS) is of considerable interest. The blood–brain barrier (BBB) plays a key regulatory role in this process by tightly controlling molecular entry into the brain [12]. The BBB's endothelial tight junctions restrict paracellular transport, allowing most small molecules to pass only through transcellular routes that depend on passive diffusion or active transporter-mediated mechanisms [13]. Passive diffusion is generally influenced by lipophilicity, polarity, and molecular size. Given its relatively high lipophilicity (logP ≈ 3.02) [14], nobiletin would be expected to cross the BBB efficiently. However, prior studies have shown that nobiletin can also modulate efflux transporters, particularly P-glycoprotein (P-gp), which may alter its disposition in the brain [15–17]. Although nobiletin has been detected in mouse brain tissue following intraperitoneal or oral administration [18–20], the detailed mechanism of its BBB transport remains insufficiently characterized. In particular, it is unclear to what extent passive diffusion or P-gp recognition determines its brain permeability. Understanding these transport pathways is critical for advancing nobiletin as a functional food bioactive and potential neuroprotective therapeutic [21]. Therefore, the present investigation aimed to clarify the mechanism of nobiletin transport across the BBB by (i) evaluating its passive diffusion using a parallel artificial membrane permeability assay (PAMPA–BBB), (ii) characterizing its P-gp substrate properties through ATPase activity and bidirectional transport assays in MDR1-overexpressing cells, and (iii) determining its plasma and brain distribution kinetics in mice in the presence and absence of the P-gp inhibitor elacridar.

MATERIALS AND METHODS

Chemicals: Nobiletin (purity >98%) along with quinidine, verapamil hydrochloride, elacridar, flavone, midazolam, and theophylline were procured from FUJIFILM Wako Pure Chemical Corporation (Osaka, Japan). Hanks' balanced salt solution (HBSS, with calcium and magnesium) and 4-(2-hydroxyethyl)-1-piperazineethanesulfonic acid (HEPES) were obtained from Thermo Fisher Scientific (Waltham, MA, USA). Fetal bovine serum (FBS) was purchased from Biowest (Nuaillé, France), and Medium 199 from Gibco (Burlington, Canada). Brain Polar Lipid Extract (porcine origin) was purchased from Avanti Polar Lipids (Alabaster, AL, USA). All other chemicals were of analytical grade and used without further purification.

PAMPA-BBB Assay: The passive diffusion capacity of nobiletin was determined using the PAMPA–BBB model following the modified method of Di et al. [22] A 96-well MultiScreen IP filter plate (Millipore, MA, USA) was coated with a lipid solution prepared by dissolving 20 mg/mL Brain Polar Lipid Extract in dodecane. Four microliters of the lipid mixture were applied to each well's filter bottom to form the artificial membrane. The

donor compartment was filled with 300 µL of the test compound solution in phosphate-buffered saline (PBS, pH 7.4), and the acceptor side with 200 µL PBS. After incubation at 37°C for 4 hours, concentrations in the acceptor phase were quantified using a POWERSCAN HT microplate reader (DS Pharma Biomedical, Osaka, Japan). The apparent permeability coefficient (Pe) was calculated using the equation:

$$P_e = -\ln(1-C_A/C_D)/(A \times (1/V_D + 1/V_A) \times t) \quad (1)$$

where C_A is the final concentration in the acceptor compartment, C_D is the initial concentration in the donor compartment, A is the effective filter area, V_D and V_A are the volumes of the donor and acceptor compartments, respectively, and t is the incubation time.

ATPase Assay: To evaluate P-gp substrate interaction, human MDR1 membrane vesicles (Genomembrane Inc., Yokohama, Japan) were utilized. Reaction mixtures contained 10 µg of membrane protein, 12 mM Mg-ATP, and 3 mM sodium orthovanadate in buffer (50 mM MOPS-Tris, 0.1 mM EGTA, 50 mM KCl, 5 mM NaN_3, 2 mM DTT, and 1 mM ouabain, pH 7.0). Test compounds (nobiletin or verapamil) were incubated at 37°C for 30 minutes, and reactions were stopped with 10% sodium dodecyl sulfate. Released inorganic phosphate was quantified spectrophotometrically at 840 nm using an eight-point calibration curve. Km and Vmax values were obtained by fitting data to the Michaelis–Menten model using GraphPad Prism 10.

Cell Culture: LLC-PK1 cells (porcine kidney epithelial cells) were obtained from JCRB Cell Bank, National Institutes of Biomedical Innovation, Health and Nutrition (Osaka, Japan). LLC-GA5-COL300 cells (LLC-PK1 cells transfected with human MDR1) were obtained from the RIKEN BioResource Center (Ibaraki, Japan). These cell lines were selected because they had the ability to form tight junctions and are suitable for evaluating P-gp-mediated transport. LLC-PK1 cells were cultured in Medium 199 containing 10% FBS, 100 units/mL penicillin, and 100 µg/mL streptomycin at 37°C in a humidified incubator under a 5% CO_2 atmosphere. Colchicine (300 ng/mL) was added to the medium for LLC-GA5-COL300 cells. LLC-PK1 and LLC-GA5-COL300 cells were thawed and subcultured every 3–4 d to prepare cell monolayers.

Bidirectional Transport Assay Across LLC-PK1 and LLC-GA5-COL300 cells: LLC-PK1 and LLC-GA5-COL300 cells were seeded into a 24-well Transwell chamber (Millicell 24, PCF 3 µm pore size, Merck Millipore Ltd.) at a density of 3.6×10^5 cells/cm^2. LLC-PK1 cells were grown in Medium 199 containing 10% FBS, 100 units/mL penicillin, and 100 µg/mL streptomycin at 37°C in a humidified incubator under a 5% CO_2 atmosphere. LLC-GA5-COL300 cells were grown in the presence of colchicine (300 ng/mL). The medium was replaced with fresh medium every 2–3 d after seeding. Colchicine-free medium was added on the 7^{th} d, with the cells being used for the transport study 6–10 d after seeding. Transepithelial electrical resistance was measured in the well before use and was found to be 100 Ω × cm^2 or more for all the wells. Apical (AP)-to-basolateral (BL) and BL-to-AP transport was evaluated. The cells were washed twice with transport buffer (HBSS containing 25 mM d-glucose and 10 mM HEPES, pH 7.4) and preincubated for 30 min in the transport buffer at 37°C. The AP- and BL-side volume was

200 and 800 µL, respectively. The transport experiments were initiated by adding a transport buffer containing the test compounds (20 µM nobiletin, 10 µM quinidine, or 10 µM verapamil) to the AP or BL side. The P-gp substrates quinidine and verapamil were used as positive controls. After a 1-, 2-, and 3-h incubation at 37°C, 100 µL aliquots were collected from the opposite side. The concentration of the test compounds was calculated as described below. AP-to-BL and BL-to-AP apparent permeability coefficients (P_{app}) were calculated using Eq. 2, as depicted below.

$$P_{app} = (dQ/dt)/(A \times C_0) \quad (2)$$

where dQ/dt is the permeability rate and A is the surface area of the filter membrane (0.3 cm^2).

The flux ratio was calculated using Eq. 3 as follows.

$$\text{Flux ratio} = P_{app,\ B\text{-}to\text{-}A}/P_{app,\ A\text{-}to\text{-}B} \quad (3)$$

where $P_{app,\ A\text{-}to\text{-}B}$ and $P_{app,\ B\text{-}to\text{-}A}$ represent the AP-to-BL and BL-to-AP apparent permeability coefficients, respectively.

Determination of the Brain-to-plasma Concentration Ratio of Nobiletin in the Presence and Absence of P-gp Inhibitors in Mice: Male ddY mice (7–9-weeks-old, 20–30 g) were purchased from Sankyo Labo Service Corporation (Tokyo, Japan). The animal experiments were approved by the Institutional Animal Care and Use Committee of Teikyo University (approval number: 22-037) and were conducted in accordance with the guidelines for animal experiments at Teikyo University. The P-gp inhibitor elacridar was administered intravenously through the tail vein at a dose of 10 mg/kg, according to previously established protocols [23]. After 15 min, a nobiletin suspension was administered orally at 50 mg/kg body weight. After 30 min of nobiletin administration, blood was collected from the inferior vena cava and centrifuged at 1500 × *g* for 10 min at 4°C to obtain plasma. Immediately after collection, the blood was refluxed and the brain was harvested. The plasma samples and brain were frozen at −80°C until use. On the day of measurement, the brain was homogenized in saline containing 1 mM EDTA to obtain a 30% brain homogenate. Nobiletin concentrations were measured as described below. An internal standard was added to the plasma and brain homogenate. Three volumes of acetonitrile were added to the plasma or brain homogenate containing the internal standard. The extract was centrifuged at 1000 × *g* for 10 min at 4°C, and the supernatant was collected. After drying, the residue was redissolved in 40% acetonitrile, and the concentration of nobiletin was measured.

Quantification of Nobiletin, Verapamil, and Quinidine: The concentrations of nobiletin, verapamil, and quinidine were determined via high-performance liquid chromatography (HPLC). HPLC was conducted on a Shimadzu HPLC system, including a system controller (CBM-20A), an online degasser (DGU-20A), a pump (LC-20AD), an autosampler (SIL-20AC), a column oven (CTO-20A), and a UV detector (SPD-20A). The injection volume was 10 µL. The analytes were separated using an Inertsil ODS-3 column (5 µm, 4.6 × 150 mm) maintained at 40°C. The mobile phase for nobiletin analysis was a water: acetonitrile (60:40, v/v) mixture, used under isocratic conditions at a flow rate of 1.0 mL/min. Nobiletin was detected by measuring the absorbance at 330 nm. For verapamil and quinidine, the mobile phase consisted of a

water: acetonitrile: methanol (60:30:10, v/v/v) mixture with 0.1 mL acetic acid and 0.2 mL triethylamine added per liter. The injection volume was 20 µL. Isocratic elution was performed at a flow rate of 1.0 mL/min with a mobile phase ratio of 60:40 (A:B). The compounds were detected by measuring the absorbance at 238 nm.

Statistical Analyses: Statistical analyses were performed using Microsoft® Excel® for Microsoft 365 MSO (Microsoft Corporation, Redmond, WA, USA) and GraphPad Prism 10 (GraphPad Software Inc., Boston, MA, USA). Data are presented as mean ± standard deviation. The Student's two-tailed *t*-test was used to analyze the significance of differences between groups in the bidirectional transport assays and *in vivo* studies. The Michaelis–Menten kinetics analysis was performed for the ATPase assay using GraphPad Prism 10. A *p*-value <0.05 was considered statistically significant.

RESULTS AND DISCUSSION

Evaluation of the Passive Transport of Nobiletin Using PAMPA-BBB: In the PAMPA–BBB model, the permeability coefficients (Pe) for low-permeability reference drugs, theophylline and scopolamine, were determined to be $0.66 \pm 0.05 \times 10^{-6}$ cm/s and $1.6 \pm 0.04 \times 10^{-6}$ cm/s, respectively. These results aligned closely with prior validation studies [24-27]. In contrast, nobiletin displayed a Pe value of $12.2 \pm 0.91 \times 10^{-6}$ cm/s, a level similar to that of verapamil ($15.1 \pm 0.42 \times 10^{-6}$ cm/s) and midazolam ($14.1 \pm 0.96 \times 10^{-6}$ cm/s)—two compounds known for efficient BBB penetration. These data confirm that nobiletin is highly permeable across lipid membranes and possesses strong passive transport capability. This is consistent with earlier observations suggesting that the compound's lipophilic structure favors efficient transcellular diffusion into the CNS.

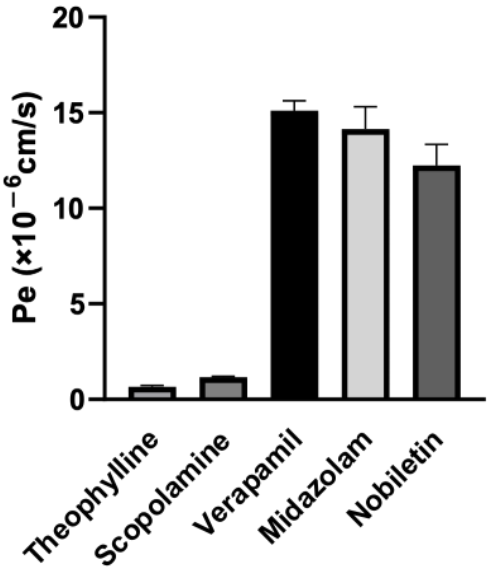

Figure 1. Passive permeability of nobiletin and reference compounds across an artificial membrane. Permeability was evaluated using the PAMPA-BBB assay. The effective permeability (P_e) values are presented as mean ± SD (n = 3). Verapamil and theophylline were used as high- and low-permeability references, respectively. Midazolam, a known CNS-active drug, was included for comparison.

P-gp Substrate Recognition and P-gp-Mediated Transport of Nobiletin: P-gp substrate involvement was assessed by measuring compound-induced changes in ATP hydrolysis using human MDR1-enriched membrane vesicles. Both nobiletin and the reference substrate verapamil produced concentration-dependent increases in ATPase activity (Figure 2). The estimated Km values were 0.816 μg/mL (2.03 μM) for nobiletin and 0.901 μg/mL (1.83 μM) for verapamil. These findings indicate that nobiletin activates P-gp ATPase with an apparent affinity similar to verapamil, consistent with its previously reported ability to modulate (inhibit) P-gp function [15–17].

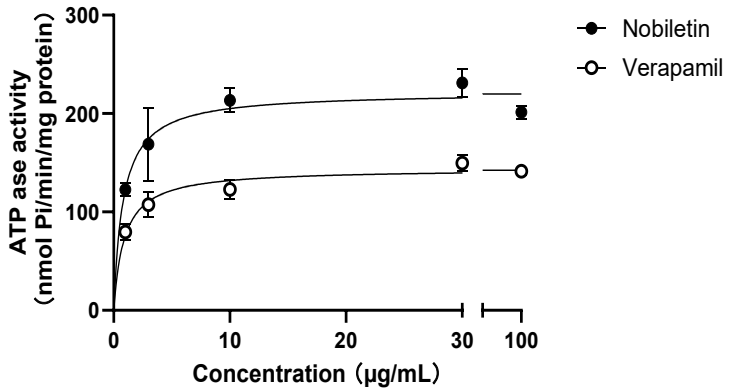

Figure 2. Effect of nobiletin and verapamil on P-gp ATPase activity. Concentration-dependent stimulation of P-gp ATPase activity by nobiletin (●) and verapamil (○). P-gp-enriched membrane vesicles were incubated with various concentrations of test compounds at 37°C for 30 min. ATPase activity was determined by measuring the amount of inorganic phosphate released. Data are expressed as mean ± SD of three independent experiments performed in triplicate.

To determine the P-gp-mediated transport of nobiletin, a bidirectional transport assay was performed using LLC-PK1 and LLC-GA5-COL300 cells, overexpressing P-gp. The transport of nobiletin, verapamil, and quinidine from AP-to-BL and BL-to-AP was increased linearly up to 3 h (Figure 3). The $P_{app, B\text{-}to\text{-}A}$ value for nobiletin, verapamil, and quinidine was significantly greater than that of the LLC-GA5-COL300 cells, respectively, whereas no significant difference was observed between the $P_{app, B\text{-}to\text{-}A}$ and $P_{app, A\text{-}to\text{-}B}$ values in LLC-PK1 cells (Table 1). The flux ratios for nobiletin, verapamil, and quinidine were 0.82, 0.99, and 0.95 in LLC-PK1 cells, and 1.54, 1.58, and 3.40 in LLC-GA5-COL300, respectively. The net flux ratios (flux ratio in LLC-GA5-COL300 cells/flux ratio in LLC-PK1 cells) for nobiletin, verapamil, and quinidine were 1.88, 1.60, and 3.58, respectively. The significant increases in BL-to-AP transport in P-gp-expressing cells indicated that nobiletin is transported by P-gp as a substrate, like verapamil, although its recognition by P-gp is weaker than that of quinidine. According to the USA Food and Drug Administration (FDA) guidelines "*In Vitro* Drug Interaction Studies—Cytochrome P450 Enzyme- and Transporter-Mediated Drug Interactions," when the net flux ratio (flux ratio in expressing cells/flux ratio in non-expressing cells) is two or greater, the risk of drug interactions as a P-gp substrate should preferably be considered and comprehensively evaluated *in vivo* [28]. In the present study, the net flux ratio for nobiletin was 1.88, which is slightly below the FDA criterion of 2.0. As a substrate of P-gp, nobiletin is not considered to be strong enough to cause clinical drug interactions mediated by P-gp.

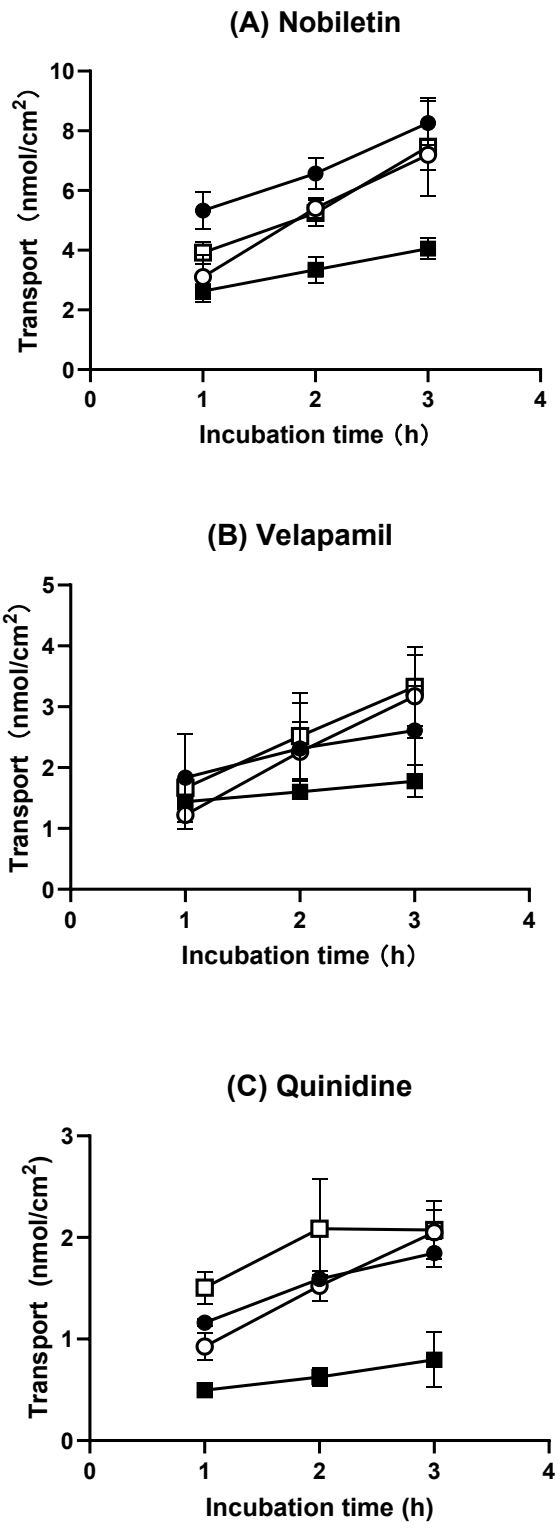

Figure 3. Time profiles for the bidirectional transport of quinidine, verapamil, and nobiletin across LLC-PK1 and LLC-GA5-COL300 cell monolayers. Time-dependent transport of (A) nobiletin (20 μM), (B) verapamil (10 μM), and (C) quinidine (10 μM) in the bidirectional transport assay. ●: AP to BL transport across LLC-PK1; ○: BL to AP transport across LLC-PK1; ■: AP to BL transport across LLC-GA5-COL300; □: BL to AP transport across LLC-GA5-COL300. Data are presented as mean ± SD (*n* = 4–5).

Table 1. Bidirectional transport assay using LLC-PK1 and LLC-GA5-COL300 cells.

	LLC-PK1 cells			LLC-GA5-COL300 cells			Net flux ratios
	$P_{app, A to B}$ (×10^{-6} cm/s)	$P_{app, B to A}$ (×10^{-6} cm/s)	Flux ratio	$P_{app, A to B}$ (×10^{-6} cm/s)	$P_{app, B to A}$ (×10^{-6} cm/s)	Flux ratio	
Nobiletin	26.2±4.44	21.5±2.75	0.82	13.4±2.92	20.7±0.78**	1.54	1.88
Verapamil	30.5±8.81	30.2±7.15	0.99	21.3±0.78	33.6±9.89*	1.58	1.60
Quinidine	25.6±2.60	24.4±2.06	0.95	10±0.98	33.9±9.99**	3.40	3.58

* $P < 0.05$, $P_{app, B to A}$ vs $P_{app, A to B}$.

** $P < 0.01$, $P_{app, B to A}$ vs $P_{app, A to B}$.

Data shown are mean ± SD (n = 4–5).

Evaluation of Brain Transport of Nobiletin in Mice and Effect of P-gp Inhibition: To evaluate in vivo brain delivery of nobiletin and determine whether P-gp inhibition alters its distribution, mouse studies were performed. After oral dosing of nobiletin (50 mg/kg), the plasma concentration increased rapidly, reaching a peak value of 2.54 ± 0.60 μg/mL at 30 min, and then declined at later time points (Figure 4A). The short time to C_{max} suggests efficient gastrointestinal absorption following oral administration. Brain concentration followed a closely matched kinetic profile, rising in parallel with plasma levels and attaining a maximum of 3.12 ± 0.96 μg/g tissue at 30 min (Figure 4B). These plasma and brain time-course patterns are consistent with prior reports [19]. The near-synchronous peaks in plasma and brain further indicate rapid distribution between the systemic circulation and brain across the BBB.

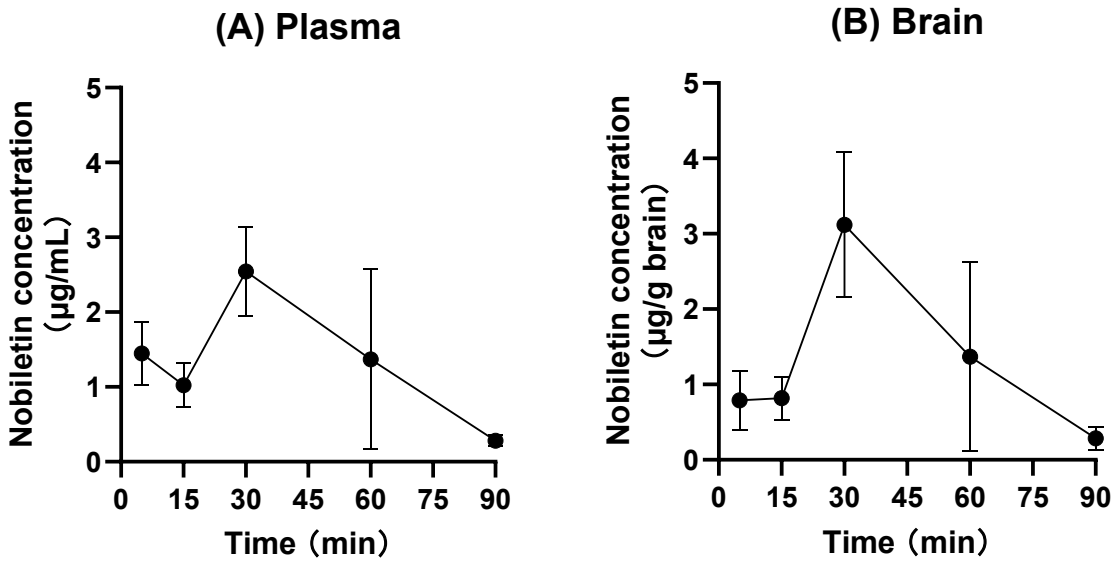

Figure 4. Time course of nobiletin concentration in the plasma and brain tissue following oral administration in mice. ddY mice were orally administered nobiletin at 50 mg/kg body weight (n = 3–4 per time point). The blood and brain samples were collected 5, 15, 30, 60, and 90 min after administration. (A) Plasma concentration of nobiletin. (B) Brain tissue concentration of nobiletin. Data are presented as mean ± SD.

To examine whether P-gp limits nobiletin entry into the brain, the impact of transporter inhibition was assessed at 30 min after dosing, corresponding to the time of maximal nobiletin exposure. Pretreatment with elacridar (administered 15 min before nobiletin) did not produce a significant change in nobiletin concentrations in either plasma or brain compared with controls ($p > 0.05$; Figure 5A, B). Likewise, the brain-to-plasma concentration ratio at 30 min was 0.73 ± 0.18 mg/mL in the control group and 0.93 ± 0.28 mg/mL in the elacridar-treated group, with no statistically significant difference between groups ($p > 0.05$; Figure 5C). It should be noted, however, that this evaluation was limited to a single time point at peak concentration (T_{max}). A more comprehensive assessment involving multiple time points and area-under-the-curve (AUC) analysis would be necessary to fully exclude the possibility that P-gp affects nobiletin distribution kinetics. Nevertheless, the absence of a significant difference in the brain/plasma ratio at T_{max} under P-gp inhibition suggests that the functional impact of P-gp on nobiletin brain transport is negligible under the tested conditions. Consistent with this interpretation, verapamil—whose lipophilicity and relatively weak P-gp substrate characteristics resemble those of nobiletin—has been reported in multiple human PET studies to show minimal sensitivity to P-gp-mediated efflux from brain to blood [29,30]. Overall, the present findings indicate that any P-gp-dependent efflux of nobiletin at the BBB is too limited to measurably affect its brain distribution, and thus coadministration with a P-gp inhibitor is unlikely to substantially alter nobiletin brain exposure.

This study addresses key steps in the Functional Food Center's (FFC) functional food development framework [31,32]. Specifically, our findings contribute to Step 5 (Bioavailability & Biokinetics) through quantification of nobiletin's passive BBB permeability and plasma/brain pharmacokinetics, and to Step 8 (Mechanism of Action) through elucidation of the relative contributions of passive diffusion and P-gp-mediated efflux to CNS distribution. By establishing that nobiletin—a bioactive compound from citrus—efficiently crosses the BBB via passive diffusion, these mechanistic insights provide critical foundational data supporting its translation toward functional food products targeting brain health outcomes, including neuroprotection and cognitive function.

To our knowledge, this study provides the first quantitative in vivo evidence that P-gp does not functionally restrict the brain distribution of nobiletin. Prior studies have either demonstrated P-gp substrate recognition in vitro or detected nobiletin in brain tissue *in vivo* [15-20], but none have directly examined whether P-gp functionally limits CNS uptake under defined pharmacokinetic conditions. The present findings address this gap by combining passive permeability quantification (PAMPA-BBB), mechanistic transporter characterization (ATPase assay and bidirectional transport), and in vivo pharmacokinetic validation in a single integrated study, establishing passive diffusion as the predominant mechanism of BBB transport for nobiletin.

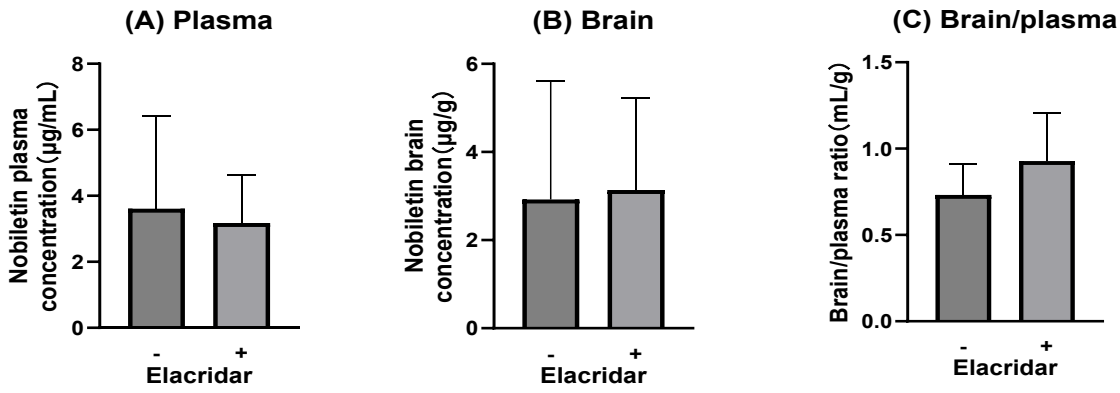

Figure 5. Effect of P-gp inhibition on nobiletin concentration in the plasma and brain as well as brain-to-plasma concentration ratio in mice. (A) Plasma concentration of nobiletin in control and elacridar-treated mice. (B) Brain concentration of nobiletin in control and elacridar-treated mice. (C) Brain-to-plasma concentration ratios of nobiletin in control and elacridar-treated mice. Mice were pretreated with vehicle (control) or elacridar (P-gp inhibitor) 15 min before nobiletin administration. Samples were collected 30 min after nobiletin dosing. Data are presented as mean ± SD (n = 8). No significant differences were observed between the control and elacridar-treated groups.

CONCLUSION

This study comprehensively clarified the mechanism by which nobiletin crosses the blood–brain barrier. Experimental evidence from PAMPA–BBB analysis confirmed that nobiletin exhibits high passive permeability, comparable to other lipophilic CNS-active compounds such as verapamil and midazolam. Although nobiletin modestly activated P-gp ATPase and showed a weak substrate-like behavior in bidirectional transport assays, its functional interaction with P-gp was limited. Pharmacokinetic evaluation in mice further demonstrated that nobiletin rapidly distributes between plasma and brain tissues following oral administration, achieving peak concentrations within 30 minutes. The absence of a significant difference in brain-to-plasma ratios after elacridar pretreatment at the time of peak concentration (30 min) indicates that P-gp inhibition does not meaningfully influence nobiletin's CNS transport under the tested conditions. Taken together, these findings establish passive diffusion as the principal route of nobiletin entry into the brain, with P-gp playing a negligible role. This insight enhances understanding of nobiletin's pharmacological potential and supports its further exploration as a neuroprotective or cognitive-enhancing bioactive component in functional food and nutraceutical applications.

List of Abbreviations: AP, apical; BL, basolateral. Biomolecules/structures—ATP, adenosine triphosphate; BBB, blood–brain barrier; P-gp, P-glycoprotein; MDR1, multidrug resistance protein 1. Reagents/buffers—FBS, fetal bovine serum; HBSS, Hanks' balanced salt solution; HEPES, 4-(2-hydroxyethyl)-1-piperazineethanesulfonic acid; PBS, phosphate-buffered saline; PS, penicillin–streptomycin. Methods/metrics—PAMPA, parallel artificial membrane permeability assay; Papp, apparent permeability coefficient; TEER, transepithelial electrical resistance; HPLC, high-performance liquid chromatography; PET, positron emission tomography. Organization—FDA, Food and Drug Administration.

Author's Contributions: E.N. contributed significantly to this study. E.N., S.T., T.Y., J.W., S.Y., and T.O. collectively designed the study. E.N. and T.O. were responsible for conducting the experiments, analyzing the data, and

writing the manuscript. The remaining authors assisted in editing the manuscript. All authors have read and consented to the final version of the manuscript.

Competing Interests The authors declare no conflict of interest.

Acknowledgement and Funding: The authors thank all laboratory members for their technical assistance and helpful discussions. This work was supported by JSPS KAKENHI Grant Number JP25K18197 (Grant-in-Aid for Early-Career Scientists).

REFERENCES

1. Chen Y.Y., Liang J.J., Wang D.L., Chen J.B., Cao J.P., Wang Y., et al.: Nobiletin as a chemopreventive natural product against cancer: a comprehensive review. *Crit Rev Food Sci Nutr.* 2023; 63:6309–6329.
DOI: https://doi.org/10.1080/10408398.2022.2030297
2. Cheng Y., Feng S., Sheng C., Yang C., Li Y.: Nobiletin from citrus peel: a promising therapeutic agent for liver disease—pharmacological characteristics, mechanisms, and potential applications. *Front Pharmacol.* 2024; 15:1354809.
DOI: https://doi.org/10.3389/fphar.2024.1354809
3. Yarim G.F., Yarim M., Sozmen M., Gokceoglu A., Ertekin A., et al.: Nobiletin attenuates inflammation via modulating proinflammatory and anti-inflammatory cytokine expressions in an autoimmune encephalomyelitis mouse model. *Fitoterapia.* 2022; 156:105099.
DOI: https://doi.org/10.1016/j.fitote.2021.105099
4. Rosas-Martínez M., Gutiérrez-Venegas G.: Comparison of Nobiletin and 5-Demethylnobiletin as Cancer Chemopreventive Agents. Eur J Cancer Care. 2024; 2024:1128095.
DOI: https://doi.org/10.1155/ecc/1128095
5. Wu Y., Cheng C.-S., Li Q., Chen J.X., Lv L.L., Xu J.Y., et al.: The application of Citrus folium in breast cancer and the mechanism of its main component, nobiletin: a systematic review. *Evid Based Complement Alternat Med.* 2021; 2021:2847466.
DOI: https://doi.org/10.1155/2021/2847466
6. Amarsanaa K., Kim H.J., Ko E.A., Jo J., Jung S.C.: Nobiletin exhibits neuroprotective effects against mitochondrial complex I inhibition via regulation of apoptotic signaling. *Exp Neurobiol.* 2021; 30:73–86.
DOI: https://doi.org/10.5607/en20051
7. Parihar A.: Nobiletin as a Neuroprotective Agent: Therapeutic Potential and Formulation Strategies for Alzheimer's and Related Disorders. J Drug Deliv Ther. 2025; 15:134–143.
DOI: https://doi.org/10.22270/jddt.v15i7.7261
8. Ghasemi-Tarie R., Kiasalari Z., Fakour M., Khorasani M., Keshtkar S., Baluchnejadmojarad T., et al.: Nobiletin prevents amyloid β1-40-induced cognitive impairment via inhibition of neuroinflammation and oxidative/nitrosative stress. *Metab Brain Dis.* 2022; 37:1337–1349.
DOI: https://doi.org/10.1007/s11011-022-00949-y
9. Xiong W., Li R., Li B., Wang X., Wang H., Sun Y., et al.: Nobiletin mitigates D-galactose-induced memory impairment via improving hippocampal neurogenesis in mice. *Nutrients*. 2023; 15:2228.
DOI: https://doi.org/10.3390/nu15092228
10. Pang Y., Xiong J., Wu Y., Ding W.: A review on recent advances on nobiletin in central and peripheral nervous system diseases. *Eur J Med Res*. 2023; 28:485.
DOI: https://doi.org/10.1186/s40001-023-01468-9
11. Yamada S., Shirai M., Ono K., Teruya T., Yamano A., Tae Woo J.: Beneficial effects of a nobiletin-rich formulated supplement of Sikwasa (C. depressa) peel on cognitive function in elderly Japanese subjects: a multicenter, randomized, double-blind, placebo-controlled study. *Food Sci Nutr*. 2021; 9:6844–6853.
DOI: https://doi.org/10.1002/fsn3.2640
12. Zhao N., Chung T.D., Guo Z., Jamieson J.J., Liang L., Linville R.M., et al.: The influence of physiological and pathological perturbations on blood–brain barrier function. *Front Neurosci.* 2023; 17:1289894.
DOI: https://doi.org/10.3389/fnins.2023.1289894
13. Wu D., Chen Q., Chen X., Han F., Chen Z., Wang Y.: The blood–brain barrier: structure, regulation and drug delivery. *Signal Transduct Target Ther.* 2023; 8:217.
DOI: https://doi.org/10.1038/s41392-023-01481-w
14. Elengoe A., Pal P., Poddar S.: Molecular computational drug design algorithms using machine learning for phytocompounds from Dimocarpus longan L. Appl NanoBioSci. 2024; 13:123.
DOI: https://doi.org/10.33263/LIANBS133.123
15. Honda Y., Ushigome F., Koyabu N., Morimoto S., Shoyama Y., Uchiumi T., et al.: Effects of grapefruit juice and orange juice components on P-glycoprotein- and MRP2-mediated drug efflux. *Br J Pharmacol*. 2004; 143:856–864.

DOI: https://doi.org/10.1038/sj.bjp.0706008

16. Ohtani H., Ikegawa T., Honda Y., Kohyama N., Morimoto S., Shoyama Y., et al.: Effects of various methoxyflavones on vincristine uptake and multidrug resistance to vincristine in P-gp-overexpressing K562/ADM cells. *Pharm Res.* 2007; 24:1936–1943.
DOI: https://doi.org/10.1007/s11095-007-9320-6
17. Ma W., Feng S., Yao X., Yuan Z., Liu L., Xie Y.: Nobiletin enhances the efficacy of chemotherapeutic agents in ABCB1-overexpressing cancer cells. *Sci Rep.* 2015; 5:18789.
DOI: https://doi.org/10.1038/srep18789
18. Toledo R., Tomás-Navarro M., Yuste J.E., Crupi P., Vallejo F.: An update on citrus polymethoxyflavones: chemistry, metabolic fate, and relevant bioactivities. Eur Food Res Technol. 2024; 250:2179–2192.
DOI: https://doi.org/10.1007/s00217-024-04529-5
19. Singh S.P., Wahajuddin, Tewari D., Patel K., Jain G.K.: Permeability determination and pharmacokinetic study of nobiletin in rat plasma and brain by validated high-performance liquid chromatography method. *Fitoterapia*. 2011; 82:1206–1214.
DOI: https://doi.org/10.1016/j.fitote.2011.08.010
20. Okuyama S., Miyazaki K., Yamada R., Amakura Y., Yoshimura M., Sawamoto A., et al.: Permeation of polymethoxyflavones into the mouse brain and their effect on MK-801-induced locomotive hyperactivity. *Int J Mol Sci.* 2017; 18:489.
DOI: https://doi.org/10.3390/ijms18030489
21. Kato R., Zhang L., Kinatukara N., Huang R., Asthana A., Weber C., et al.: Investigating blood–brain barrier penetration and neurotoxicity of natural products for central nervous system drug development. Sci Rep. 2025; 15:7431.
DOI: https://doi.org/10.1038/s41598-025-90888-2
22. Di L., Kerns E.H., Fan K., McConnell O.J., Carter G.T. High-throughput artificial membrane permeability assay for blood–brain barrier. *Eur J Med Chem.* 2003; 38:223–232.
DOI: https://doi.org/10.1016/S0223-5234(03)00012-6
23. Cox B., Nicolaï J., Williamson B. The role of the efflux transporter, P-glycoprotein, at the blood-brain barrier in drug discovery. Biopharm Drug Dispos. 2023; 44:113–126.
DOI: https://doi.org/10.1002/bdd.2331
24. Árpád Könczöl, Judit Müller, Emília Földes, Zoltán Béni, Krisztina Végh, Ágnes Kéry, et al. Applicability of a Blood–Brain Barrier Specific Artificial Membrane Permeability Assay at the Early Stage of Natural Product-Based CNS Drug Discovery. *J. Nat. Prod.* 2013, 76, 4, 655–663.
DOI: https://doi.org/10.1021/np300882f
25. Bicker J., Alves G., Fortuna A., Soares-da-Silva P., Falcão A. A new PAMPA model using an in-house brain lipid extract for screening the blood–brain barrier permeability of drug candidates. *Int J Pharm.* 2016; 501:102–111.
DOI: https://doi.org/10.1016/j.ijpharm.2016.01.074
26. Liew K.F., Hanapi N.A., Chan K.L., Yusof S.R., Lee C.Y. Assessment of the blood–brain barrier permeability of potential neuroprotective aurones in parallel artificial membrane permeability assay and porcine brain endothelial cell models. *J Pharm Sci.* 2017; 106:502–510.
DOI: https://doi.org/10.1016/j.xphs.2016.10.006
27. Shimazu R., Anada M., Miyaguchi A., Nomi Y., Matsumoto H. Evaluation of blood–brain barrier permeability of polyphenols, anthocyanins, and their metabolites. *J Agric Food Chem*. 2021; 69:11676–11686.
DOI: https://doi.org/10.1021/acs.jafc.1c02898
28. FDA Guidance for Industry. In vitro drug interaction studies: cytochrome P450 enzyme- and transporter-mediated drug interactions. U.S. Food and Drug Administration. 2020. Retrieved on February 26, 2026, https://www.fda.gov/media/134582/download
29. Muzi M., Mankoff D.A., Link J.M., Shoner S, Collier A.C., Sasongko L, et al. Imaging of cyclosporine inhibition of P-glycoprotein activity using 11C-verapamil in the brain: studies of healthy humans. *J Nucl Med.* 2009; 50:1267–1275.
DOI: https://doi.org/10.2967/jnumed.108.059162
30. Eyal S., Ke B, Link J.M., Mankoff D.A., Collier A.C., et al. Regional P-glycoprotein activity and inhibition at the human blood–brain barrier as imaged by positron emission tomography. *Clin Pharmacol Ther.* 2010; 87:579–585.
DOI: https://doi.org/10.1038/clpt.2010.11
31. Martirosyan D.M., Alvarado A. Functional Foods Regulation System: Proposed Regulatory and Labeling Guidelines. *Funct Food Sci.* 2023; 3:275–287.
DOI: https://doi.org/10.31989/ffs.v3i11.1265
32. Martirosyan D.M. Functional Food Science in the era of artificial intelligence: The role of domain authority, structured validation, and responsible translation. *Funct Food Sci.* 2026; 6:104–114.
DOI: https://doi.org/10.31989/ffs.v6i2.1903